ChemComm

Accepted Manuscript

ROYAL SOCIETY OF CHEMISTRY

rsc.li/chemcomm

View Article Online
DOI: 10.1039/C8CC05982A

Journal Name

COMMUNICATION

Increasing Time on Target: Utilization of Inhibitors of Cysteine Cathepsins to Enhance the Tumor Retention of Receptor-Targeted Agents

Received 00th January 20xx,
Accepted 00th January 20xx

DOI: 10.1039/x0xx00000x

www.rsc.org/

Wei Fan, †[ab], Wenting Zhang,†[ab] Sameer Alshehri, [ab] and Jered C. Garrison *[abcd]

We report a strategy of utilizing irreversible cysteine cathepsin inhibitor as trapping agent to increase the tumor residence time of receptor-targeted agents. The targeted constructs incorporating these cysteine cathepsin trapping agents were able to form high molecular weight adducts with intracellular cysteine cathepsins, thus achieving superior retention in tumor tissues.

The development of receptor-targeted radiopharmaceuticals that selectively bind to overexpressed receptor populations in cancerous tissues has been, and continues to be, extensively investigated.[1] The targeting constructs for these agents can be broadly divided into carriers of low-molecular weight (*e.g.*, small molecules and peptides) and high-molecular weight (*e.g.*, proteins and antibodies). Low-molecular weight carriers offer several advantages relative to macromolecules, such as rapid accumulation in the target and clearance from non-target sites.[2] Unfortunately, compared to high-molecular weight carriers, smaller molecules generally have inherently higher metabolism and diffusion characteristics, leading to decreased tumor residence times that often diminish translational potential, particularly for therapeutic applications.

Cysteine cathepsins (CCs) are a family of 11 endolysosomal proteases with a variety of functions, but are primarily attributed to protein catabolism.[3] These proteases are highly expressed (*i.e.,* mM) in endolysosomal compartments, but are also known to exist extracellularly. The extracellular activity of CCs is generally very low and tightly regulated in normal tissue through a number of biological mechanisms.[4] In cancers, however, upregulation of both the expression and activity of CCs has been observed[5] and has garnered interest in the development of reversible and irreversible inhibitors of these proteases for diagnostic and therapeutic purposes.[6]

Dipeptidyl acyloxymethyl ketones (AOMKs) are one example of a class of irreversible inhibitors for CCs.[7] These inhibitors have high selectivity for the active site of CCs. They can also form irreversible thioether linkages with the cysteine responsible for the catalytic function of the protease.[8a] To date, a variety of AOMK inhibitors has been reported for diagnostic and therapeutic purposes related to cysteine cathepsins known role in cancer.[7a, 8]

Herein, we propose a synergistic concept that utilizes CC inhibitors, such as AOMKs, as novel and powerful CC-trapping agents (CCTAs) to improve the retention of low-molecular weight, receptor-targeted radiopharmaceuticals (Figure 1A).

Upon binding of the agonistic-targeting vector to its corresponding cellularreceptor and intracellular trafficking to the endolysosomal compartments, we hypothesized that targeting vectors incorporating these CCTAs can irreversibly bind to the highly expressed and active CCs within these compartments. As a result, high-molecular weight, intracellular CC-adducts, which would limit cellular efflux and diffusion of the radiopharmaceutical were expected, thereby enhancing its long-term retention in target tissues. It was anticipated that by using this strategy, significant increases in the target/non-target (T/NT) ratios could be achieved, thereby increasing the likelihood of clinical translation. To examine the utility of this concept, the neurotensin (NT) peptide / NTSR1 was utilized as the model platform, a system for which our laboratory is well versed.[9]

NTSR1 is a receptor known to be overexpressed in a number of cancers, including pancreatic, prostate, and colon[2a, 10]. In this study, the synthesized NTSR1-targeted agents utilizes an NT fragment (*i.e.,* NT(6-13)) as the targeting vector. This peptide has a low-molecular weight with nanomolar binding affinity to the NTSR1. Figure 1 provides a schematic outlining the synthesized NTSR1-targeted conjugates. Briefly, the AOMK

[a] *Department of Pharmaceutical Sciences, University of Nebraska Medical Center, 985830 Nebraska Medical Center, Omaha, NE 68198, United States.*
[b] *Center for Drug Delivery and Nanomedicine, University of Nebraska Medical Center, 985830 Nebraska Medical Center, Omaha, NE 68198, United States.*
[c] *Department of Biochemistry and Molecular Biology, University of Nebraska Medical Center, 985870 Nebraska Medical Center, Omaha, NE 68198, United States*
[d] *Eppley Cancer Center, University of Nebraska Medical Center, 985950 Nebraska Medical Center, Omaha, NE 68198, United States.*
† These authors contributed equally to this work.
Electronic Supplementary Information (ESI) available: [details of any supplementary information available should be included here]. See DOI: 10.1039/x0xx00000x

View Article Online
DOI: 10.1039/C8CC05982A

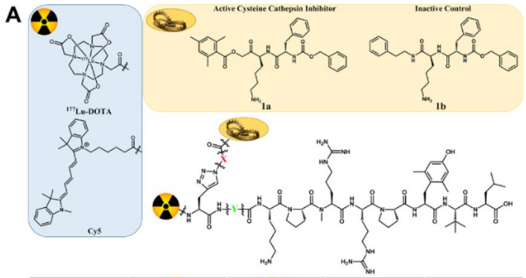

B

Compound			X	Y
2a	^{177}Lu-DOTA	1a	Null	β-Ala
2b	^{177}Lu-DOTA	1a	Acetyl	β-Ala
2c	^{177}Lu-DOTA	1a	PEG_3	β-Ala
2d	^{177}Lu-DOTA	1a	Gly-$(D)Ser_3$	β-Ala
2e	^{177}Lu-DOTA	1a	PEG_3	$(D)Ser_3$
2f	^{177}Lu-DOTA	1a	Gly-$(D)Ser_3$	$(D)Ser_3$
3a	^{177}Lu-DOTA	1b	PEG_3	β-Ala
3b	^{177}Lu-DOTA	1b	Gly-$(D)Ser_3$	$(D)Ser_3$
4a	Cy5	1a	Gly-$(D)Ser_3$	$(D)Ser_3$
4b	Cy5	1b	Gly-$(D)Ser_3$	$(D)Ser_3$

Fig. 1 (A) Scheme outlining the structure of the CCTA-incorporated, NTSR1-targeted analogs. (B) Table detailing the structural components of the synthesized analogs. ^{177}Lu-DOTA – lutetium-177-labeled-1,4,7,10-tetraazacyclododecane-1,4,7,10-tetraacetic acid; Cy5 – Cyanine 5; PEG3 - 2-[2-[2-(2-azidoethoxy)ethoxy]ethoxy]acetic acid.

inhibitor 1a was utilized as the model CCTA and the non-reactive 1b (no inhibition) was used as a structurally analogous control. The lutetium-177 (^{177}Lu)-labeled-conjugates 2a-2d were used to access the impact of the CCTA linker (X) on the activity of the radioconjugate. For radioconjugates 2e-2f, modifications were made to the peptide (Y) and the CCTA linker to examine how increases in hydrophilicity impacted biological performance. Radioconjugates 3a-3b utilized the inactive CCTA (1b) and served as matching controls to the experimental analogs. Lastly, a fluorescent dye (Cyanine 5, Cy5) was conjugated to the CCTA-incorporated peptide to yield the experimental compound 4a, with 4b serving as the matched control. Synthetic schemes and details regarding the synthesis of these compounds can be found in the supporting information. The ^{177}Lu radiolabeling efficiencies of the conjugates were determined to be from 54.5 % to 88.8 % (Figure S1 and S2). No radiolysis was detected under the radiolabeling condition for all the conjugates.

To assess the *in vitro* CC-trapping potency of these conjugates, the inhibition constant of the conjugates relative to the unmodified inhibitor 1a were determined. Cathepsin B (CatB) was chosen as the model CC due to its ubiquitous expression in mammalian cells and the selectivity of 1a for this protease. By monitoring the initial hydrolysis rates of the substrate by CatB at different concentrations in the presence of the conjugates (Figure S4), the observed rate constant (K_{obs}) was calculated and converted to the inhibition constants (K_i) (Figure S4, S5 and S6) according to the determined Michaelis-Menten constant (K_m) of the CatB (Figure S3). The results showed that only the hydrophilic CCTA conjugates (2a-2f) demonstrated low nanomolar Ki and inhibition IC_{50} to CatB, similar to the 1a control (Table 1 and Table S4 and S5). As expected, the unlabeled control analogs of 3a and 3b did not demonstrate any inhibition over the concentrations investigated. In addition, the NTSR1-binding affinity of the conjugates was investigated using a competitive binding assay with HT-29 human colon cancer cells, a well-known NTSR1-positive cell line[9a]. All of the conjugates exhibited comparable nanomolar binding affinities

Table 1 The Log $D_{7.4}$, CatB inhibition constant, and competitive binding (IC_{50}) to NTR1 of the compounds

Compound	Log$D_{7.4}$	CatB K_i (nM)	NTSR1 IC_{50} (nM)
1a	2.08 ± 0.08[a]	23 ± 1	–
1b	2.51 ± 0.02[a]	ni[c]	–
2a	-1.46 ± 0.02[b]	25 ± 4	20 ± 2
2b	-1.49 ± 0.02[b]	26 ± 5	22 ± 2
2c	-0.98 ± 0.02[b]	69 ± 13	19 ± 1
2d	-1.79 ± 0.06[b]	73 ± 8	20 ± 3
2e	-1.71 ± 0.05[b]	72 ± 2	20 ± 3
2f	-1.95 ± 0.05[b]	50 ± 13	18 ± 2
3a	-1.56 ± 0.07[b]	ni	49 ± 5
3b	-2.01 ± 0.06[b]	ni	52 ± 8

[a] The Log $D_{7.4}$ was determined by HPLC analysis. [b] The Log $D_{7.4}$ was determined by radiometric analysis. [c] No inhibition observed.

(Table 1). These results suggest minimal impact of the CCTA on the conjugate affinity for the NTSR1 and vice versa (*i.e.,* the impact of the peptide on the CCTA efficacy).

Efflux studies were performed to examine the HT-29 cellular retention profile of the radioconjugates over a 24 h period, as shown in Figure 2A. Increased retention was observed as the CCTA linker (X) increased in length from null (2a) to acetyl (2b) to PEG_3 (2c), suggesting the length impacts the cellular activity. Unexpectedly, the longest linker Gly-$(D)Ser_3$ (2d), did not follow this trend and had a cellular retention profile similar to 2a. However, introduction of a $(D)Ser_3$ in the peptide linker (Y) resulted in a substantial increase in the cellular retention of the analogous 2f. This data implies that introducing a PEG linker between the CCTA and the peptide or inserting a three-D-Serine linker in the peptide sequence could benefit the intracellular binding of the conjugates.

Compound 2c exhibited substantially reduced efflux (36%) compared to the structurally analogous inactive CCTA control 3a (66%) at 24 h. Similarly, 2f yielded reduced efflux results

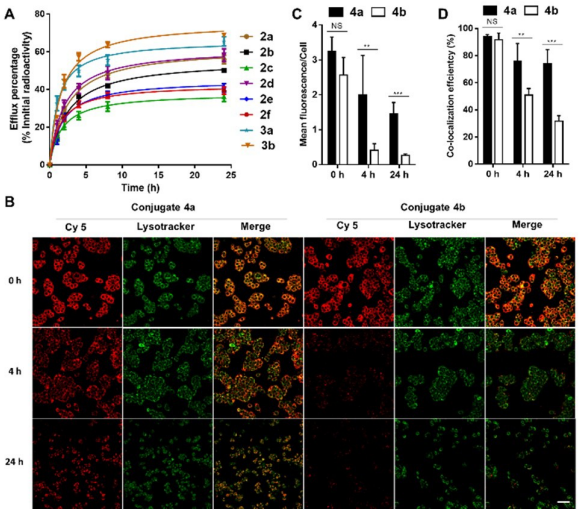

Fig. 2. (A) Efflux of the internalized 2a-f and 3a-b in HT-29 cells, values are means ± SD (n = 3). (B) Representative confocal microscopy images of the efflux of Cy5 labeled 4a and 4b (red) formHT-29 cells. Cell endolysosomal compartments were stained with Lysotracker (green). Scale bar = 50 μm. (C) Time-dependent fluorescence intensity of Cy5 per cell as quantified from the confocal images. (D) Co-localization efficiency of Cy5 (red) overlapping with Lysotracker (green). All the analysis was performed in 6 random images and were presented as mean ± SD. **p < 0.01, ***p < 0.001, NS = not significant.

View Article Online
DOI: 10.1039/C8CC05982A

(39%) relative to 3b (69%). The percentage surface bound vs internalization of 2c and 2f (Figure S7) was also investigated. The surface bond for both of the conjugates was observed to be significantly (4 - 5 fold) higher than that of our previous NTSR1 ligand at 2h,[9b] which is likely due to the increased hydrophobicity after the incorporation of the CCTAs. Overall, the inclusion of an active CCTA into the NTR1-targeted peptide construct led to a clear increase in cellular retention.

The cell trafficking study of the Cy5-labeled conjugate 4a and its CCTA-inactive counterpart 4b was carried out utilizing confocal microscopy. The conjugates were efficiently internalized by the cells within 2 h, providing strong fluorescence intensity (red) in the cytoplasm (Figure S8 and S9). This internalization could be effectively blocked by the addition of an unlabeled NTSR1-targeted agent, demonstrating that the cellular uptake is NTSR1-mediated. The co-localization of the Cy5 signal of conjugates 4a or 4b with the LysoTracker™ (green) signal indicated intracellular trafficking by the endolysosomal pathway. The intracellular retention of the conjugates was further investigated over time (Figure 2B). The incorporation of CCTA significantly prolonged the residence time of 4a in the cells, imparting a 5.5 fold increase in florescence compared with its inactive counterpart, conjugate 4b at 24 h (Figure 2C). Remarkably, in contrast to 4b, the co-localization of 4a within the endolysosomal compartments (LysoTracker™ signal) persisted throughout the 24 h time period (Figure 2D). These observations strongly suggest the CCTA in 4a enabled the CC-mediated trapping of this conjugate in the endolysosomal compartments.

To examine the ability of conjugates 2f and 2c to form macromolecular adducts with CCs, gel permeation chromatography (GPC) and sodium dodecyl sulfate polyacrylamide gel electrophoresis (SDS-PAGE) were utilized.

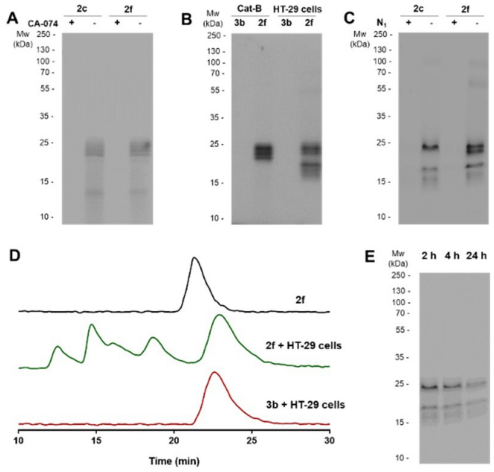

Fig.3. (A) The autoradiography of the SDS-PAGE showing the cathepsin B binding of the conjugates can be completely inhibited by cysteine proteases inhibitor CA-074. (B) The autoradiography of the SDS-PAGE gel from the CatB and live HT-29 cell samples after incubation with 2f and 3b. (C) The autoradiography of the SDS-PAGE demonstrated that co-incubation with competitive NTSR1 ligand N_1 could result in the significant inhibition of the intracellular adduct formation of the conjugates. (D) The GPC profiles of 2f and HT-29 cells samples after incubation with 2f and 3b. (E) Autoradiographic image of a SDS-PAGE gel examining the time-dependent retention of CatB-conjugate adducts in HT-29 cells after pre-incubation with 2f for 4 h.

Indeed, co-incubation with CA-074 (Figure 3A), a CatB selective inhibitor,[11] eliminated observable CatB adducts. No interference on CatB binding of the conjugates was observed when co-incubated with the competitive NTSR1 ligand confirmed the minimal impact of the NTSR1 peptide on affinity of the conjugates to CatB (Figure S10A). These CCTA-incorporated conjugates have been shown to bind to the Cys-29 residue[12] in the active site of the protease. Autoradiographic SDS-PAGE demonstrated adduct formation of 2f (Figure 3B) and 2c (Figures S10B) with CatB (~24 kDa heavy chain). Incubation of 2f and 2c in live HT-29 cells resulted in multiple macromolecule adducts formed, including CatB and possibly other cysteine cathepsin adducts. In addition, the intracellular adduct formation of the conjugates was found to be substantially inhibited by the co-incubation with a competitive NTSR1 ligand (Figure 3C), indicating that adduct formation is dependent on receptor-mediated endocytosis.

The intracellular adduct formation was also confirmed by the observation of multiple adducts in the GPC analysis (Figure 3D and Figure S11). Based on the GPC profile, the percentages of macromolecular adducts, with respect to total intracellular activity, were calculated as 61% for 2c and 66% for 2f, indicating that the radioconjugates efficiently bind to CCs after internalization. Furthermore, the radiolabeled adducts of 2f could still be detected by SDS-PAGE after 24 h (Figure 3E), suggesting a significant portion of these adducts are able to remain intact over this timespan. Quantification of the radioactive signal from the SDS-PAGE experiments revealed that signal at 24 h was 51%, relative to 2 h, suggesting that the half-life of these cellular adducts is approximately 24 h. As expected, the inactive controls (3a and 3b) demonstrated no adduct formation by either technique.

The excellent serum stability (Figure S12 and S13) and more hydrophilic profile (Table 1) of 2f prompted the examination of the *in vivo* targeting and retention profiles of this agent. Using an HT-29 xenograft mouse model, the biodistribution profile of 2f and the inactive control 3b, were determined (Table S5). Both conjugates demonstrated good muscle and blood clearance. Tumor uptake (Figure 4A) of the two radioconjugates was statistically identical at 4 hours. However, by 24 hours, 2f had a 25% increase in tumor uptake, while the tumor retention of 3b decreased significantly by 40%. Percent decreases of about 33% were seen for both conjugates at 72 h. Overall, 2f demonstrated a nearly two-fold increase in retention time in the tumors, compared to the control 3b after 24 h. Uptake in the liver and kidney were substantial for both conjugates; however, conjugate 2f demonstrated significantly increased retention compared to the CCTA-inactive 3b. The uptake in the liver is likely due to hepatic clearance and non-specific internalization of these rather lipophilic conjugates.[9a, 13] We have found (data not shown) that the liver and spleen uptake of similar CCTA-incorporated NTR1-targeted agents can be eliminated by simply increasing the hydrophilicity of the utilized agent. Renal uptake is most likely due to the well-known renal reuptake/non-specific internalization mechanism of charged peptides by the proximal tubule cells during renal excretion.[14] Given this, it is probable

View Article Online
DOI: 10.1039/C8CC05982A

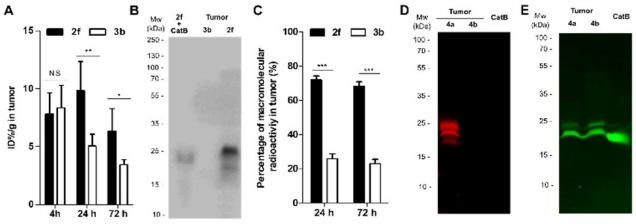

Fig.4. (A) The %ID/g in HT-29 xenograft tumors at 4, 24 and 72 h postinjection of 2f and 3b in mice (n = 5). (B) The autoradiography of SDS-PAGE of the HT-29 xenograft tumors at 24 h postinjection of 2f and 3b in mice. (C) Percentage of the macromolecule associated radioactivity (Mw > 10 kDa) in tumor tissues after administration of 2f and 3b (n=3). *p < 0.05, **p < 0.01, ***p < 0.001, NS = not significant. (D) and (E) The western blot of cathepsin B (human Liver) and the tumor homogenates after injected with 4a and 4b. The transferring membrane was stained by cathepsin B antibody and visualized by fluorescence with excitation at 635 nm (D) for Cy 5 and at 532 nm (E) for Alexa Fluor 488 of the secondary antibody.

that 2f forms adducts in the liver and kidney in a manner similar to the internalization mechanism for NTSR1-positive tumors.

To confirm this hypothesis, SDS-PAGE analysis was performed on tumor (Figure 4B) as well as liver and kidney (Figure S14) samples ex vivo for conjugates 2f and 3b. For 2f, identical adduct profiles were observed in the tumor and non-target tissue samples. These results suggest that these agents form macromolecular adducts in these tissues most likely due to the same CC-trapping mechanism. Control conjugate 3b demonstrated no signs of adduct formation. In addition, using centrifugal filtration (10 kDa MWCO) to separate macromolecules from low-molecular weight compounds, greater than 68% of the radioactivity resident in the HT-29 tumor tissues was found to be associated with macromolecules (Figure 4C) at 24 and 72 h for 2f, indicating that the increased retention in these tumors is indeed due to the CC binding. Lastly, Cy5-labeled conjugates 4a and 4b were injected into mice to further evaluate in vivo adduct formation. Similar to the biodistribution data for the radioconjugates, the ex vivo imaging results indicated that the tumor retention of 4a was greater than its counterpart 4b at 24 hours (Figure S15). Analysis of the fluorescently labeled proteins by western blot at 532 nm (Figure 4D) showed that 4a, based on corresponding CatB antibody staining (Figure 4E), was mainly bound to CatB in tumor tissues. This is thought to be due to the high CatB expression/activity profiles in cells as well as the CatB selectivity of the CCTA trapping agent.[7, 15]

In summary, this study reinforces the concept that synergistic incorporation of CC inhibitors (i.e., CCTAs) into a NTSR1-targeted peptide can lead to the ability to efficiently form adducts in the endolysosomal compartments of NTSR1-positive cells. Furthermore, the formation of these macromolecular adducts substantially prolonged the *in vivo* retention of the radioconjugates in NTSR1-positive tumors. This strategy has the potential to provide an unprecedented means to enhance the efficacy of NTR1-targeted agents for an array of diagnostic and therapeutic applications. Also, this technology is expected to be easily adaptable to a range of receptor-avid small molecules, peptides, and other targeted agents to improve the selective retention of these agents, thereby leading to substantial improvements in translational potential.

We thank Janice A. Taylor and James R. Talaska from the Advanced Microscopy Core Facility at the UNMC for providing assistance with confocal microscopy. In addition, we gratefully acknowledge Ed Ezell at the Nuclear Magnetic Resonance (NMR) Core Facility at UNMC for assistance in collecting NMR data. We thank Melody A. Montgomery for the professional editing of this manuscript. Lastly, we acknowledge Dr. Shaheen Ahmed for providing technical support with western blot studies. This study was supported by grants from the Nebraska Department of Health and Human Services (2017-21) and the National Institutes of Health (1R01CA17905901A1).

Conflicts of interest

There are no conflicts to declare

Notes and references

1 M. J. Welch and W. C. Eckelman, *Targeted Molecular Imaging*, Taylor & Francis, Oxfordshire, 2012
2 (a) M. Fani, H. R. Maecke and S. M. Okarvi, *Theranostics*, 2012, 2, 481; (b) A. J. Fischman, J. W. Babich and H. W. Strauss, *J. Nucl. Med.*, 1993, 34, 2253; (c) S. M. Okarvi, *Cancer Treat. Rev.* 2008, 34, 13.
3 (a) J. Reiser, B. Adair and T. Reinheckel, *J. Clin. Investig.*, 2010, 120, 3421; (b) C. Palermo and J. A. Joyce, *Trends Pharmacol. Sci.*, 2008, 29, 22.
4 V. Turk, V. Stoka, O. Vasiljeva, M. Renko, T. Sun, B. Turk and D. Turk, *Biochim. Biophys. Acta,* 2012, 1824, 68.
5 (a) J. A. Joyce and D. Hanahan, *Cell Cycle*, 2004, 3, 1516; (b) N. Aggarwal and B. F. Sloane, *Proteomics Clin. Appl.*, 2014, 8, 427.
6 (a) J. Kos, A. Mitrović and B. Mirković, *Future Med. Chem.*, 2014, 6, 1355; (b) D. R. Sudhan and D. W. Siemann, *Pharmacol. Ther.*, 2015, 155, 105; (c) S. J. Salpeter, Y. Pozniak, E. Merquiol, Y. Ben-Nun, T. Geiger and G. Blum, *Oncogene*, 2015, 34, 6066.
7 (a) A. Krantz, L. J. Copp, P. J. Coles, R. A. Smith and S. B. Heard, *Biochemistry*, 1991, 30, 4678; (b) B. M. Wagner, R. A. Smith, P. J. Coles, L. J. Copp, M. J. Ernest and A. Krantz, *J. Med. Chem.*, 1994, 37, 1833.
8 (a) J. C. Powers, J. L. Asgian, Ö. D. Ekici and K. E. James, *Chem. Rev.*, 2002, 102, 4639; (b) H. H. Otto and T. Schirmeister, *Chem. Rev.*, 1997, 97, 133; (c) L. O. Ofori, N. P. Withana, T. R. Prestwood, M. Verdoes, J. J. Brady, M. M. Winslow, J. Sorger and M. Bogyo, *ACS Chem Biol*, 2015, 10, 1977.
9 (a) Y. Jia, W. Zhang, W. Fan, S. Brusnahan and J. Garrison, *Bioconjugate Chem.*, 2016, 27, 2658; (b) Y. Jia, W. Shi, Z. Zhou, N. K. Wagh, W. Fan, S. K. Brusnahan and J. C. Garrison, *Nucl. Med. Biol.*, 2015, 42, 816.
10 (a) Z. Wu, D. Martinez-Fong, J. Trédaniel and P. Forgez, *Front. Endocrinol.*, 2012, 3, 184; (b) R. M. Myers, J. W. Shearman, M. O. Kitching, A. Ramos-Montoya, D. E. Neal and S. V. Ley, *ACS Chem Biol*, 2009, 4, 503.
11 T. Towatari, T. Nikawa, M. Murata, C. Yokoo, M. Tamai, K. Hanada and N. Katunuma, *FEBS Lett.*, 1991, 280, 311.
12 G. Blum, G. von Degenfeld, M. J. Merchant, H. M. Blau and M. Bogyo, *Nat Chem Biol*, 2007, 3, 668.
13 K. L. Audus and T. J. Raub, *Biological Barriers to Protein Delivery*, Springer, Boston, 1993
14 E. Vegt, M. Melis, A. Eek, M. de Visser, M. Brom, W. J. Oyen, M. Gotthardt, M. de Jong and O. C. Boerman, Eur. *J. Nucl. Med. Mol. Imaging*, 2011, 38, 623
15 D. Kato, K. M. Boatright, A. B. Berger, T. Nazif, G. Blum, C. Ryan, K. A. Chehade, G. S. Salvesen and M. Bogyo, *Nat. Chem. Biol.*, 2005, 1, 33.

View Article Online
DOI: 10.1039/C8CC05982A

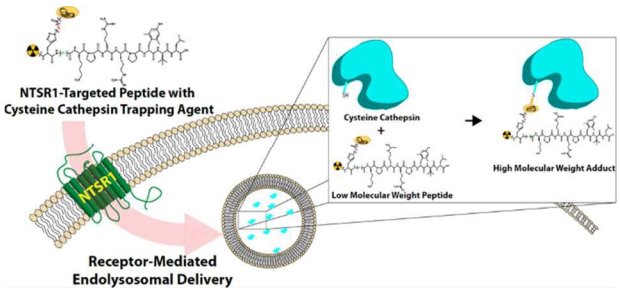

An efficient strategy of utilizing cysteine cathepsin inhibitor for enhanced tumor residence of the receptor-targeted agents was presented.